

## Original Article

# Lovastatin restores the function of endothelial progenitor cells damaged by oxLDL

Feng-xia MA, Fang CHEN, Qian REN, Zhong-chao HAN\*

State Key Laboratory of Experimental Hematology, Institute of Hematology, Chinese Academy of Medical Sciences, Tianjin 300020, China

**Aim:** The aim of the study was to investigate whether lovastatin restores the survival and function of endothelial progenitor cells (EPCs) damaged by oxLDL.

**Methods:** EPCs were preincubated with different concentrations of lovastatin (2, 10, and 50  $\mu\text{mol/L}$ ) with or without the Akt inhibitor triciribine for 24 h and were then exposed to 50  $\mu\text{g/mL}$  oxLDL for 48 h. The survival of EPCs, as well as the cellular migration, adhesion, and tube formation of these cells, was examined. To explore the mechanisms of lovastatin's effects on EPCs, the levels of phosphorylated Akt and eNOS and of total eNOS protein and mRNA were assayed.

**Results:** Incubation of EPCs with oxLDL resulted in significant apoptosis and impaired cellular migration, adhesion and tube structure formation. The detrimental effects of oxLDL on EPC survival and function were attenuated by pretreatment of EPCs with lovastatin. However, when EPCs were pretreated with lovastatin and triciribine at the same time, the beneficial effects of lovastatin were abolished by triciribine. Furthermore, oxLDL caused a significant downregulation of eNOS mRNA and protein expression, as well as a suppression of Akt and eNOS phosphorylation. However, the effects of oxLDL on Akt/eNOS activity and eNOS expression were reversed by lovastatin.

**Conclusion:** Lovastatin reverses the survival and function of EPCs by regulating the Akt/eNOS signaling pathway and the gene transcription of eNOS.

**Keywords:** oxidized low density lipoprotein; endothelial progenitor cells; endothelial nitric oxide synthase  
*Acta Pharmacologica Sinica* (2009) 30: 545–552; doi: 10.1038/aps.2009.41

## Introduction

Postnatal neovascularization is a crucial compensatory response in chronic ischemic diseases. Recently, increasing numbers of studies have indicated that postnatal neovascularization is involved in the incorporation of endothelial progenitor cells (EPCs)<sup>[1,2]</sup>. Therefore, understanding the regulation of EPCs and their mechanisms may provide new insights into therapeutic neovascularization. Our group and others have investigated the detrimental effects of oxLDL, a risk factor for cardiovascular disease, on the number and activity of EPCs<sup>[3,4]</sup>. HMG-CoA reductase inhibitors (statins) have been developed as lipid-lowering drugs and have been documented to reduce the morbidity and mortality of coronary artery disease (CAD)<sup>[5]</sup>. To gain further insight into the mechanisms by which statins improve cardiovascular function, we investigated whether statins inhibited the

detrimental effects of oxLDL on EPCs.

Recent studies have demonstrated that vascular endothelial growth factor (VEGF) and statins activate the serine/threonine kinase Akt in EPCs and induce the mobilization of bone marrow-derived EPCs<sup>[6,7]</sup>. Akt serves as a multifunctional regulator of cell biology<sup>[8]</sup>. Phosphorylated Akt becomes available to phosphorylate its downstream substrates, such as endothelial nitric oxide synthase (eNOS), leading to eNOS activation<sup>[9]</sup>. Furthermore, recent studies have suggested that eNOS serves as a significant regulator of hemangioblast activity<sup>[10]</sup>. Thus, we hypothesize that the Akt/eNOS signaling pathway is involved in the effects of statins on the biology of EPCs.

## Materials and methods

**Preparation and oxidation of LDL** Written informed consent was obtained from all volunteers in accordance with the institutional Ethics Committee. Blood samples for LDL preparation were taken from healthy volunteers after 12 h of

\* Correspondence to Prof Zhong-chao HAN.  
E-mail tihzchan@public.tpt.tj.cn  
Received 2008-11-09 Accepted 2009-03-18

fasting. LDL was separated by density gradient ultracentrifugation. The purity of the LDL was determined by agarose gel electrophoresis and the protein content was determined by the modified Lowry method. LDL was oxidized by exposure to  $\text{CuSO}_4$ . EDTA was then added, and the sample was dialyzed against PBS to stop the oxidation process. Compared with LDL, oxidized LDL showed increased electrophoretic mobility in agarose gels and had higher concentrations of thiobarbituric acid reactive substances.

**Culture and identification of EPCs** Mononuclear cells (MNCs) were isolated by histopaque-density gradient centrifugation within 4 h of human umbilical cord blood collection. Written informed consent was obtained from all mothers in accordance with the institutional Ethics Committee.  $\text{CD34}^+$  cells were isolated from MNCs with the CD34 Isolation Kit (MACS, Miltenyi Biotec) according to the manufacturer's instructions.  $\text{CD34}^+$  cells were seeded in fibronectin-coated culture flasks (Invitrogen) and cultured in endothelial cell growth medium-2 (EGM-2) (Clonetics) supplemented with 50 ng/mL vascular endothelial growth factor (VEGF, Pepro Tech), 100 ng/mL stem cell growth factor (SCF, Pepro Tech), and 20 ng/mL interleukin-3 (IL-3, kindly provided by Kirin Pharmaceuticals). After 7–10 d of culture, non-adherent cells were removed.

To examine the expression of surface markers on EPCs, cells were incubated with monoclonal mouse anti-human antibodies against VE-cadherin or vWF (BD PharMingen) for 30 min at 4 °C. Cells were further incubated with fluorescein isothiocyanate (FITC)-conjugated rat anti-mouse IgG. For additional analysis, cells were incubated for 30 min at 4 °C with phycoerythrin (PE)-conjugated mouse anti-human CD133 (Miltenyi Biotec) or FITC-conjugated mouse anti-human CD34, CD31, CD106, and CD14 antibodies (BD PharMingen). Isotype-matched antibodies served as a control. The cells were then fixed in 1% polyformaldehyde and quantitatively analyzed with a flow cytometer (Becton Dickinson).

EPCs were incubated with 10  $\mu\text{g}/\text{mL}$  Dil Ac-LDL (Molecular Probes) at 37 °C for 4 h and fixed with 2% paraformaldehyde for 10 min. Cells were washed and then incubated with 10  $\mu\text{g}/\text{mL}$  FITC-UEA-1 (Sigma) at 4 °C for 30 min. The incorporation of Ac-LDL and the binding of UEA-1 were detected with a fluorescent microscope (Leica Microsystems, GmbH).

**Treatment of EPCs** Except for the control cells, EPCs were stimulated with 50  $\mu\text{g}/\text{mL}$  oxLDL for 48 h. Samples of the EPCs were preincubated with different concentrations of lovastatin (2, 10, and 50  $\mu\text{mol}/\text{L}$ ) for 24 h and then exposed to oxLDL for 48 h. To determine the role of Akt in the pro-

cess, EPCs were co-incubated with 50  $\mu\text{mol}/\text{L}$  lovastatin and 1  $\mu\text{mol}/\text{L}$  triciribine for 24 h and then exposed to oxLDL for 48 h.

**Apoptosis assay** For *in situ* detection of apoptotic cells, EPCs were fixed with 2% paraformaldehyde. Then, a terminal deoxynucleotidyl transferase-mediated dUTP nick end labeling (TUNEL) assay was applied according to the manufacturer's instructions (Roche Molecular Biochemicals); The EPCs were counterstained with DAPI (Sigma). TUNEL positive cells were examined in a blinded fashion and the percentage of TUNEL positive cells was evaluated.

**Adhesion assay** After detachment and centrifugation, EPCs were resuspended in adhesion buffer (0.5% BSA in EBM-2). Identical numbers of cells were replated onto fibronectin-coated culture plates, incubated for 30 min at 37 °C, and then carefully washed three times with adhesion buffer to remove non-adherent cells. The adherent cells were stained with Dil Ac-LDL and counted under a fluorescence microscope at a 200 $\times$  magnification by independent blinded investigators. Six independent fields were assessed for each well, and the average number of adherent cells/200 $\times$ field was determined.

**Migration assay** The migration of EPCs was performed in a Transwell Chamber (Corning Costar). In brief, EPCs were gently detached, harvested and resuspended in chemotaxis buffer (EBM-2, 0.5% BSA). Chemotaxis buffer (100  $\mu\text{L}$ ) containing  $1 \times 10^5$  cells was added to the upper compartment and 600  $\mu\text{L}$  of chemotaxis buffer with 100 ng/mL VEGF was added to the lower compartment. After incubation at 37 °C for 4 h, the filters were removed and the cells in the lower compartment were counted using flow cytometry with appropriate gating for 20 s at a high flow rate. Chemotaxis buffer (600  $\mu\text{L}$ ) with  $1 \times 10^5$  cells was also counted in the same way as the standard. The migratory rate was determined by calculating the percentage of the input cells that migrated into the lower chamber divided by the number of input cells originally added to the upper compartment ( $1 \times 10^5$ ). All groups of experiments were studied in triplicate.

**Tube formation assay** ECM gel (Sigma) was thawed at 4 °C overnight and placed in a 96-well culture plate at 37 °C for 1 h to allow for solidification. EPCs were harvested and replated (10 000 cells/well) on top of the solidified ECM gel in EBM-2 medium supplemented with 0.5% BSA and VEGF (100 ng/mL). Cells were incubated at 37 °C for 24 h. Tube formation was defined as a structure exhibiting a length four times its width. The networks of tubes were photographed from six randomly chosen fields under a microscope. The total length of the tube structures in each photograph was

measured using Adobe Photoshop software.

### Semiquantitative reverse transcription-PCR

Total RNA was extracted from EPCs using the RNA extraction kit (Qiagen). To generate cDNA, RNA (250 ng) was reverse transcribed with reverse transcriptase. For PCR amplification, two specific primers were used to identify and amplify eNOS (sense primer: 5'-ATGAAGCACCTGGAGAATGAG-3'; antisense primer: 5'-TCGGAGCCATACAGGATTG-3'). The PCR product was 299 bp. For PCR, 30 cycles were used at 94 °C for 40 s, 50 °C for 1 min and 72 °C for 1 min. The reverse transcription PCR-amplified samples were visualized on 1% agarose gels using ethidium bromide. Each mRNA band was normalized with internal reference  $\beta$ -actin mRNA. Bands of interest were analyzed by scan analysis software and normalized to  $\beta$ -actin mRNA bands.

**Western blot analysis** EPC lysates were separated by sodium dodecyl sulfate-polyacrylamide gel electrophoresis (SDS-PAGE) and transferred to polyvinylidene difluoride membranes (Millipore). The membranes were blocked by incubation in Tris-buffered saline [10 mmol/L Tris (pH 7.5), 100 mmol/L NaCl] containing 0.1% (*v/v*) Tween 20 and 5% (*v/v*) non-fat dry milk for 2 h, followed by incubation at room temperature with rabbit polyclonal antiphospho-Akt-Ser 473 and eNOS-Ser1177 antibodies (Cell Signaling Technology) or mouse monoclonal anti-eNOS antibodies (BD Transduction Laboratories) for 2 h. The membranes were washed extensively in Tris-buffered saline containing 0.1% (*v/v*) Tween 20 before incubation for 1 h with a horseradish peroxidase-conjugated anti-mouse or anti-rabbit secondary antibody (Amersham Life Sciences). The membranes were then washed and developed using enhanced chemiluminescence (ECL) substrate (Amersham Life Sciences). The membranes were reprobbed with an anti-actin antibody (Santa Cruz Biotechnology) or an anti-Akt antibody (Cell Signaling Technology).

**Statistical analysis** Data were expressed as means $\pm$ SD. Differences between group means were determined by a one-way ANOVA, followed by a Newman-Keuls test.  $P < 0.05$  was considered statistically significant.

## Results

**The identification of EPCs** After the CD34<sup>+</sup> cells were sorted twice by immunomagnetic sorting with a CD34 antibody, the purity of enriched CD34<sup>+</sup> cells was higher than 90% (Figure 1A). When CD34<sup>+</sup> cells were cultured on fibronectin-coated dishes, many cell clusters appeared and numerous spindle-shape cells sprouted from the edge of

the cell clusters after cultivation for 4–7 d. Flow cytometric analysis revealed that the ratio of CD31 expression was 67% $\pm$ 7%, the ratio of VE-cadherin expression was 70% $\pm$ 3%, and the ratio of vWF expression was 47% $\pm$ 5%. The expression levels of CD14, CD106, and CD45 were very low. The stem cell marker CD133 was still expressed by the EPCs (Figure 1B). To confirm that the cells isolated were EPCs, cells were double stained with CD31 and VE-cadherin or CD31 and CD45. Of the total cellular pool, 65% $\pm$ 8% of cells stained positively for CD31 and VE-cadherin; however, few cells were stained with both CD31 and CD45 (Figure 1C). EPCs took up Dil Ac-LDL and bound FITC-UEA-1 (Figure 1D), indicating that they expressed the scavenger receptor of Ac-LDL and the ligand of UEA-1.

**The effect of lovastatin on EPC apoptosis** EPC apoptosis was examined by *in situ* TUNEL assay, in which TUNEL-positive cells were labeled with FITC and total adherent cells were dyed blue (Figure 2A). The percentage of apoptotic cells significantly increased when EPCs were exposed to 50  $\mu$ g/mL oxLDL (oxLDL group: 21.12% $\pm$ 1.32% versus the control group, 8.99% $\pm$ 1.09%;  $P < 0.05$ ). The percentage of cells that became apoptotic in response to oxLDL was dose-dependently reduced when EPCs were pretreated with lovastatin (2, 10, and 50  $\mu$ mol/L lovastatin group: 17.92% $\pm$ 1.54%, 13.63% $\pm$ 1.87%, 9.07% $\pm$ 0.63% versus the oxLDL group;  $P < 0.05$ ). However, the percentage of apoptotic cells was increased when EPCs were pretreated with lovastatin and triciniribine at the same time (50  $\mu$ mol/L lovastatin+triciniribine group: 19.12% $\pm$ 2.64% *vs* control;  $P < 0.05$ ) (Figure 2B).

**The effect of lovastatin on EPC adhesion** Adhesion of EPCs to extracellular matrix proteins is important for the formation of new blood vessels. EPCs treated with oxLDL showed a significant reduction in adhesion to fibronectin (oxLDL group: 27 $\pm$ 2 *vs* control group: 37 $\pm$ 5;  $P < 0.05$ ). When EPCs were pretreated with 2, 10, and 50  $\mu$ mol/L lovastatin, adherent cells were partially or completely restored to the level of the control (2, 10, and 50  $\mu$ mol/L lovastatin group: 32 $\pm$ 2, 38 $\pm$ 2, and 39 $\pm$ 2 *vs* oxLDL group;  $P < 0.05$ ). However, when EPCs were pretreated with lovastatin and triciniribine at the same time, the beneficial effect of lovastatin on EPC adhesion was abolished (50  $\mu$ mol/L lovastatin+triciniribine group: 27 $\pm$ 2 *vs* 50  $\mu$ mol/L lovastatin group;  $P < 0.05$ ) (Figure 3A and B).

**The effect of lovastatin on EPC migration** We analyzed the migratory activity of EPCs in response to VEGF. Figure 4 shows a significant reduction in EPC migration after treatment with oxLDL (oxLDL group: 5.0% $\pm$ 0.6% *vs* the control group: 9.6% $\pm$ 0.9%;  $P < 0.05$ ). Pretreatment of

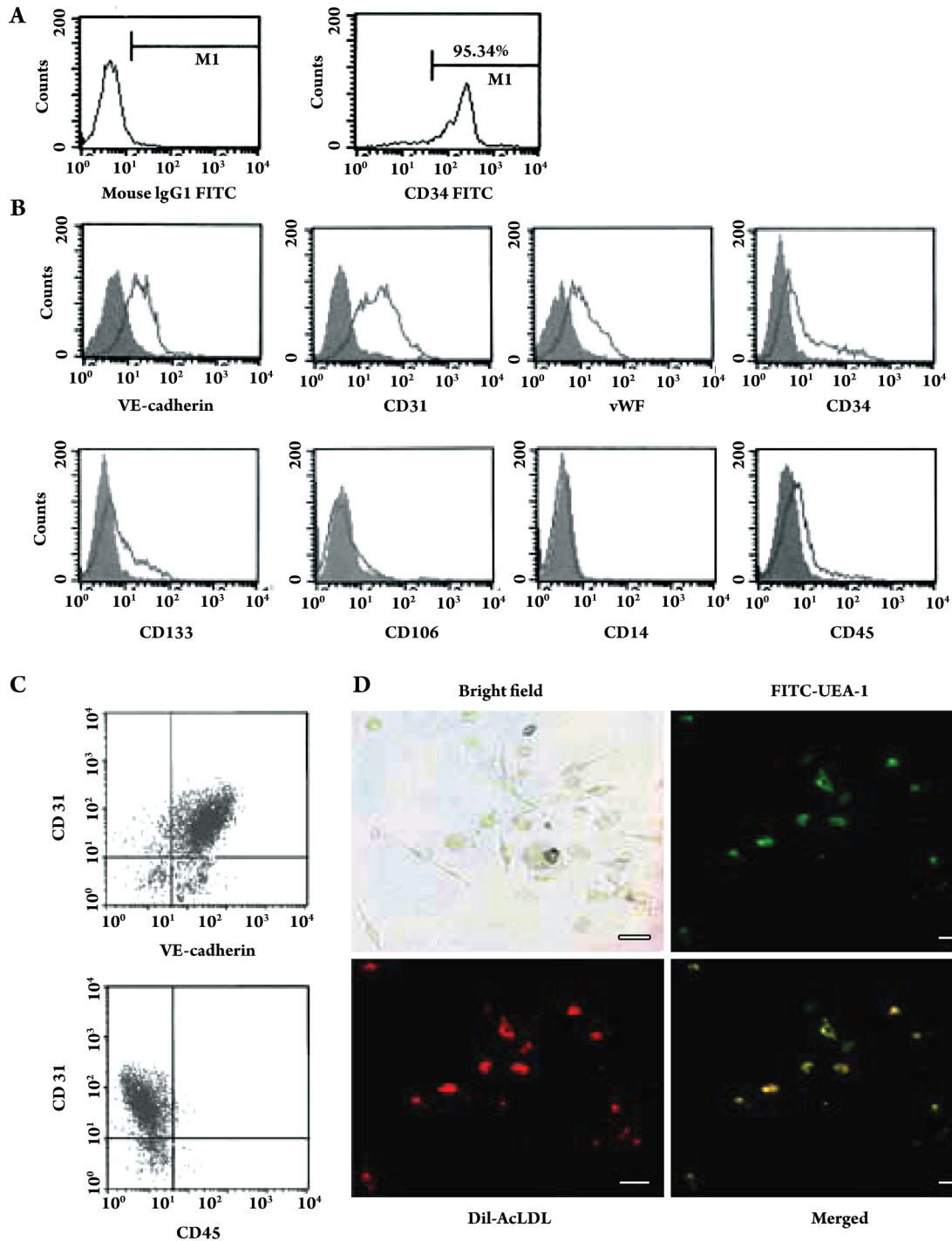


**Figure 1.** Identification of EPCs developed from cord blood CD34<sup>+</sup> cells. The purification of CD34<sup>+</sup> cells after immunomagnetic sorting (A). Representative results of flow cytometric analysis of cell markers on EPCs (B, C). Adherent cell Dil-AcLDL uptake and FITC-UEA-1 binding were determined by fluorescent microscopy. Double-positive cells, which appeared yellow in the overlay, were identified as differentiating EPCs (D). White bars: 10  $\mu$ m.

EPCs with lovastatin markedly inhibited the reduction of EPC migration in response to oxLDL (2, 10, and 50  $\mu$ mol/L

lovastatin groups: 6.8% $\pm$ 0.7%, 9.5% $\pm$ 0.7%, and 10.0% $\pm$ 0.6% vs oxLDL;  $P < 0.05$ ). However, when triciribine was added,

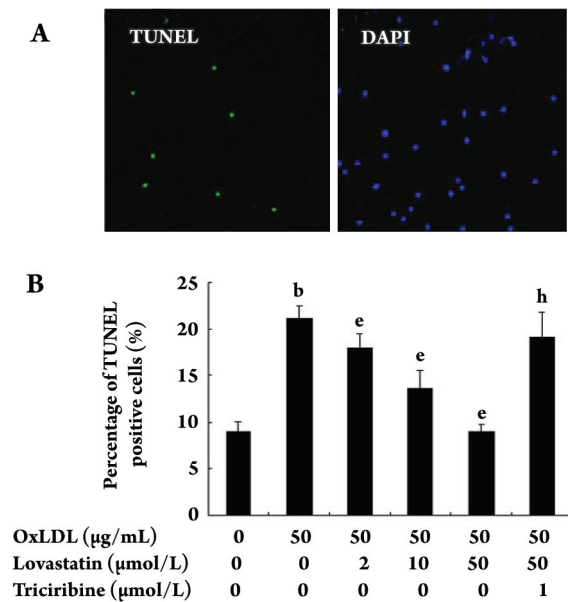


**Figure 2.** Effects of lovastatin on EPC apoptosis. An *in situ* TUNEL assay was applied to examine EPC apoptosis. FITC labeled cells are TUNEL positive and apoptotic cells, and DAPI was used to dye all the nuclei blue (A). Treatment of EPCs with oxLDL induced EPC apoptosis. Pretreatment of EPCs with lovastatin inhibited oxLDL-induced EPC apoptosis (B).  $n=10$ . Mean $\pm$ SD. <sup>b</sup> $P<0.05$  vs control. <sup>e</sup> $P<0.05$  vs oxLDL. <sup>h</sup> $P<0.05$  vs 50 μmol/L lovastatin+oxLDL.

the beneficial effect of lovastatin was abolished (50 μmol/L lovastatin+triciribine group:  $4.9\pm 0.5$  vs 50 μmol/L lovastatin group;  $P<0.05$ ) (Figure 4).

**The effect of lovastatin on EPC tube formation** EPCs incubated on matrigel for 24 h formed an extensive and enclosed tube network. OxLDL impaired the ability of EPCs to form this tube network (Figure 5A). The total length of the tube network in each photograph was decreased (oxLDL group:  $2.1\pm 0.4$  mm vs control group:  $4.6\pm 0.6$  mm;  $P<0.05$ ). Furthermore, the tube network was severely disrupted, resulting in an incomplete and sparse tube network. Lovastatin restored the ability of EPCs to form a tube network (2, 10, and 50 μmol/L lovastatin groups:  $3.2\pm 0.2$ ,  $4.5\pm 0.6$ , and  $4.8\pm 0.4$  mm vs oxLDL group;  $P<0.05$ ). Triciribine abolished the effect of lovastatin (50 μmol/L lovastatin+triciribine group:  $2.1\pm 0.4$  mm vs 50 μmol/L lovastatin group;  $P<0.05$ ) (Figure 5B).

**Regulation of eNOS mRNA expression by lovastatin** We set the eNOS mRNA expression of the control equal to 100%. Figure 6 depicts a significant downregulation of eNOS mRNA expression when EPCs were incubated with oxLDL (oxLDL group:  $41\pm 5\%$  vs control: 100%;  $P<0.05$ ). Lovastatin dose-dependently upregulated eNOS mRNA expression (2, 10, and 50 μmol/L lovastatin groups:

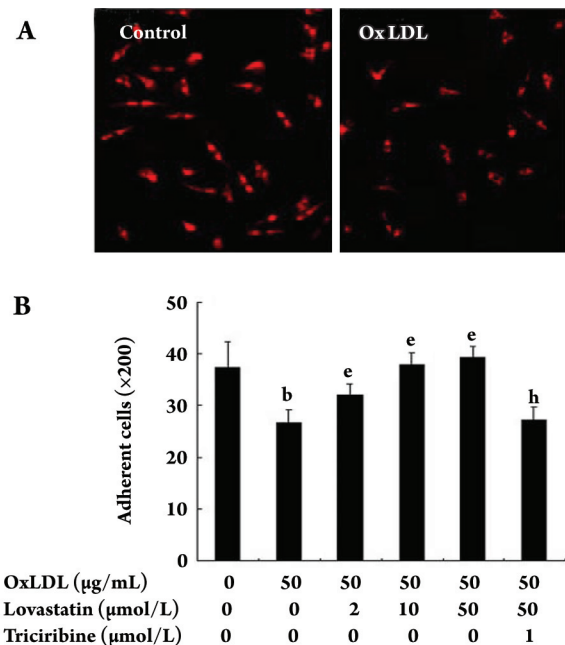


**Figure 3.** Effects of lovastatin on EPC adhesion. Identical numbers of cells were replated onto fibronectin-coated culture plates. After removal of non-adherent cells, the adherent cells were counted. Representative pictures of adherent EPCs treated with or without 50 μg/mL oxLDL are shown (A). Treatment of EPCs with oxLDL decreased EPC adhesion. Pretreatment of EPCs with lovastatin increased EPC adhesion in a dose-dependent manner (B).  $n=10$ . Mean $\pm$ SD. <sup>b</sup> $P<0.05$  vs control. <sup>e</sup> $P<0.05$  vs oxLDL. <sup>h</sup> $P<0.05$  vs 50 μmol/L lovastatin+oxLDL.

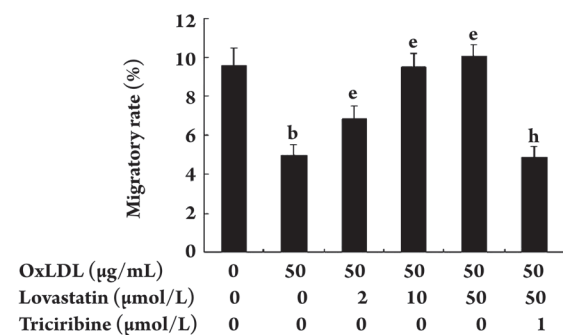


**Figure 4.** Effects of lovastatin on EPC migration. Treatment of EPCs with oxLDL decreased EPC migration. Pretreatment of EPCs with lovastatin increased EPC migration in a dose-dependent manner.  $n=8$ . Mean $\pm$ SD. <sup>b</sup> $P<0.05$  vs control. <sup>e</sup> $P<0.05$  vs oxLDL. <sup>h</sup> $P<0.05$  vs 50 μmol/L lovastatin+oxLDL.

$57\pm 5\%$ ,  $91\pm 6\%$ , and  $106\pm 9\%$  vs oxLDL group;  $P<0.05$ )

**Regulation of Akt and eNOS phosphorylation by lovastatin** To test our hypothesis that lovastatin influenced EPC activity through the Akt/eNOS pathway, immunoblots

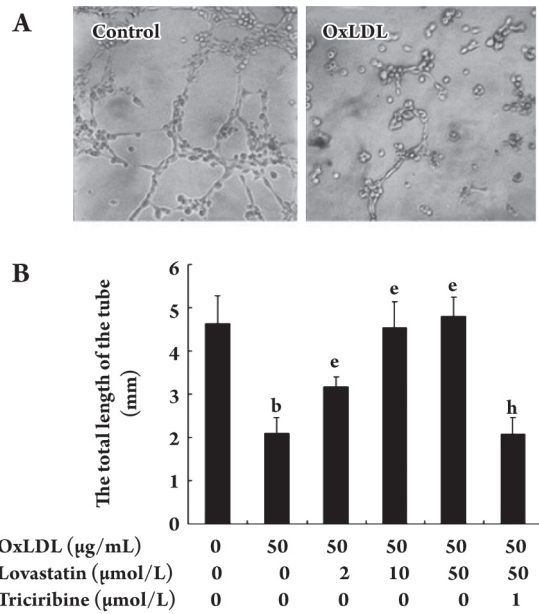


**Figure 5.** Effects of lovastatin on EPC tube formation. Representative pictures of the tube formation of EPCs treated with or without 50 µg/mL oxLDL are shown (A). Treatment of EPCs with oxLDL decreased EPC tube formation. Pretreatment of EPCs with lovastatin increased EPC tube formation in a dose-dependent manner (B). *n*=6. Mean±SD. <sup>b</sup>*P*<0.05 vs control. <sup>c</sup>*P*<0.05 vs oxLDL. <sup>h</sup>*P*<0.05 vs 50 µmol/L lovastatin.

were performed. OxLDL induced a downregulation of Akt phosphorylation (oxLDL group: 36%±3% vs control: 100%; *P*<0.05). However, lovastatin restored the phosphorylation of Akt (2, 10, and 50 µmol/L lovastatin group: 59%±7%, 91%±4%, and 98%±6% vs oxLDL group; *P*<0.05) (Figure 7).

To determine whether lovastatin influenced eNOS protein expression, eNOS protein was also assayed by immunoblots. Incubation of EPCs with oxLDL reduced eNOS protein expression (oxLDL group: 42%±7% vs control: 100%; *P*<0.05). Lovastatin (10 or 50 µmol/L) inhibited the downregulation of eNOS protein (10 and 50 µmol/L lovastatin groups: 93%±4% and 105%±6% vs oxLDL group; *P*<0.05) (Figure 8A, 8B).

To further test our hypothesis that lovastatin influenced EPC activity through the Akt/eNOS pathway, the expression of phosphorylated eNOS at the Ser1177 phosphorylation site was tested. Because the level of eNOS protein was regulated by oxLDL and lovastatin, different amounts of total protein were applied to make the eNOS protein levels similar among groups. OxLDL also reduced eNOS phosphorylation (oxLDL group: 51%±8% vs control: 100%; *P*<0.05). Lovastatin (10 or 50 µmol/L) inhibited the downregulation

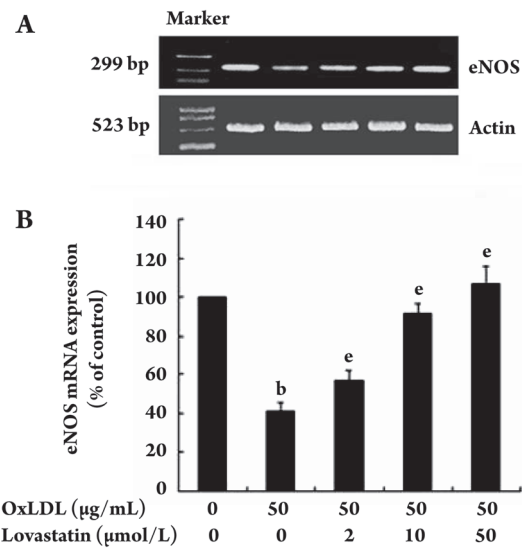


**Figure 6.** Effects of lovastatin on eNOS mRNA expression. Treatment of EPCs with oxLDL decreased eNOS mRNA expression. Pretreatment of EPCs with lovastatin inhibited oxLDL-induced downregulation of eNOS mRNA expression. Representative picture of agarose gel electrophoresis (A). The summary of data of eNOS mRNA expression (B). *n*=6. Mean±SD. <sup>b</sup>*P*<0.05 vs control. <sup>e</sup>*P*<0.05 vs oxLDL.

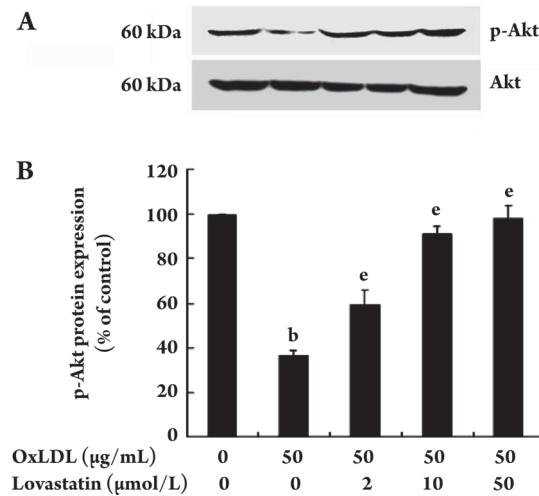


**Figure 7.** Effects of lovastatin on Akt phosphorylation. OxLDL decreased Akt phosphorylation, but pretreatment with lovastatin inhibited the decrease of Akt phosphorylation. Representative blots of Akt phosphorylation (A). Summary of data of Akt phosphorylation (B). *n*=3. Mean±SD. <sup>b</sup>*P*<0.05 vs control. <sup>e</sup>*P*<0.05 vs oxLDL.

of eNOS phosphorylation (10 and 50 µmol/L lovastatin groups: 93%±5% and 101%±4% vs oxLDL group; *P*<0.05) (Figure 8C, 8D).

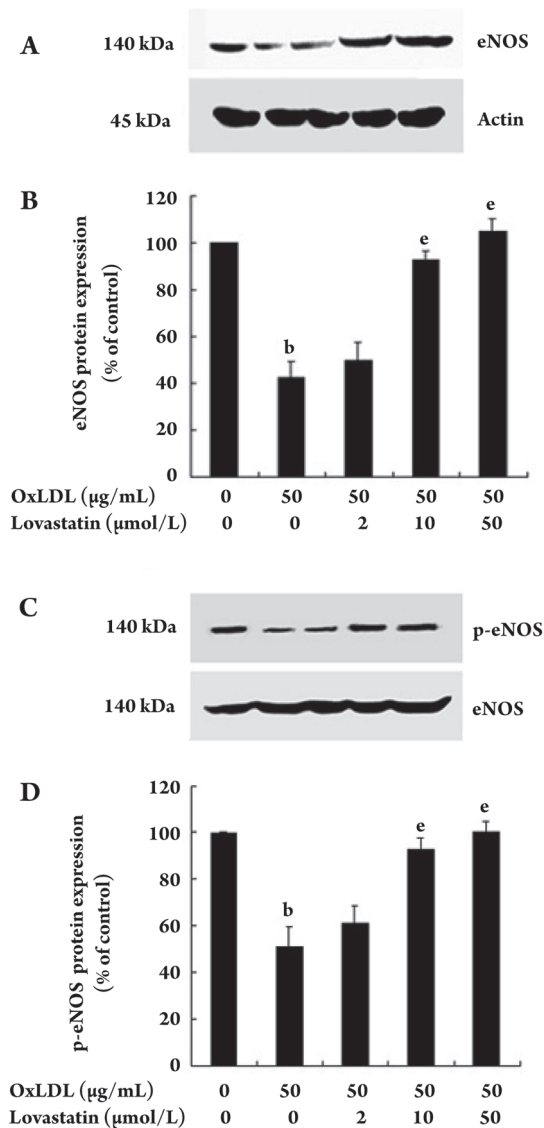


**Figure 8.** Effects of lovastatin on eNOS and p-eNOS protein expression. OxLDL decreased eNOS and p-eNOS protein expression, but pretreatment with lovastatin inhibited the downregulation of eNOS and p-eNOS protein expression. Representative blots of eNOS and p-eNOS protein (A, C). Summary of data of eNOS and p-eNOS protein expression (B, D).  $n=3$ . Mean $\pm$ SD. <sup>b</sup> $P<0.05$  vs control. <sup>e</sup> $P<0.05$  vs oxLDL.

## Discussion

Recent experimental and clinical studies have indicated that statins, widely used cholesterol-lowering drugs, possess cholesterol-independent effects<sup>[11]</sup>. The data from the present study establishes novel cholesterol-independent effects of lovastatin, augmenting EPC numbers and promoting EPC migratory, adhesive, and tube formation capacities. It has

been previously shown that atorvastatin inhibits EPC senescence and increases EPC proliferation<sup>[12]</sup>. Thus, statins have multiple protective effects on EPCs. These findings explain why the number and function of circulating EPCs was augmented by statin therapy in patients with stable CAD<sup>[13]</sup>. Circulating EPCs serve as a biological marker for vascular function and participate in neovascularization following ischemic injury<sup>[1,14]</sup>. Therefore, augmentation of circulating EPC numbers and function by statins might be a novel strategy to improve neovascularization after tissue ischemia.

Another contribution of the study was to explore the mechanisms by which lovastatin exerted protective effects on EPCs. Activation of Akt plays a central role in the biology of EPCs, promoting the survival and mobilization of EPCs<sup>[7,15]</sup>. The present results suggest that Akt is also involved in the effects of lovastatin on EPCs. Phosphorylated Akt is available to phosphorylate eNOS at Ser 1177, leading to eNOS activation in mature endothelial cells<sup>[9]</sup>. eNOS is also activated by phosphorylated Akt in EPCs. The activation of eNOS catalyzes nitric oxide (NO) generation, which plays a key role in maintaining cardiovascular homeostasis. NO is a significant regulator of EPC activity. Mice deficient in eNOS display impaired ischemia-induced angiogenesis and have reduced EPC mobilization<sup>[16]</sup>. Estrogen also increases EPC number by inducing NO generation<sup>[17]</sup>. Previous studies have shown that many downstream targets of Akt are involved in cell survival pathways, including GSK-3, BAD, NF- $\kappa$ B, and the FKHR family of forkhead transcriptional factors<sup>[18]</sup>. Indeed, the forkhead transcription factor AFX (FOXO4) is expressed in EPCs and is inactivated by statins<sup>[12]</sup>. Therefore, other targets of Akt, such as FOXO4, might play a role in the effects of lovastatin. AMPK also phosphorylates eNOS at Ser 1177<sup>[19]</sup>, leading to eNOS activation. Furthermore, the activity of eNOS is regulated by caveolin-1<sup>[20]</sup>. Whether AMPK and caveolin-1 are involved in the effects of lovastatin on EPCs needs to be explored.

On the other hand, lovastatin up-regulated eNOS mRNA and protein expression. These findings not only suggest that activation of the Akt/eNOS pathway is involved in causing the effects of lovastatin, but also that increased gene transcription of eNOS is involved. Statins upregulate eNOS by blocking Rho geranylgeranylation and by increasing the stability of eNOS mRNA<sup>[21]</sup>, which could explain why lovastatin upregulated the gene transcription of eNOS.

In conclusion, the results of the present study demonstrate that treatment of EPCs with lovastatin significantly reverses the detrimental effects of oxLDL on the survival and function of EPCs through activation of the Akt/eNOS pathway and induction of eNOS gene transcription. Statins had

pleiotropic protective effects on EPCs through *via* multiple mechanisms. Given the well-established role of EPCs in vessel repair after ischemic injury, statins might be therapeutically useful to promote the vasculogenesis in ischemic tissue, even in patients with normal cholesterol levels.

### Acknowledgements

This work was supported by the National High Technology Research and Development Program of China (No 2006AA02A110).

### Author contribution

Zhong-chao HAN and Feng-xia MA designed the research; Feng-xia MA, Fang CHEN and Qian REN performed the research; Fang CHEN and Qian REN contributed analytic reagents and tools; Feng-xia MA analyzed the data; Zhong-chao HAN and Feng-xia MA wrote the paper.

### References

- Asahara T, Masuda H, Takahashi T, Kalka C, Pastore C, Silver M, *et al*. Bone marrow origin of endothelial progenitor cells responsible for postnatal vasculogenesis in physiological and pathological neovascularization. *Circ Res* 1999; 85: 221–8.
- Murayama T, Tepper OM, Silver M, Ma H, Losordo DW, Isner JM, *et al*. Determination of bone marrow-derived endothelial progenitor cell significance in angiogenic growth factor-induced neovascularization *in vivo*. *Exp Hematol* 2002; 30: 967–72.
- Ma FX, Zhou B, Chen Z, Ren Q, Lu SH, Sawamura T, *et al*. Oxidized low density lipoprotein impairs endothelial progenitor cells by regulation of endothelial nitric oxide synthase. *J Lipid Res* 2006; 47: 1227–37.
- Imanishi T, Hano T, Sawamura T, Nishio I. Oxidized low-density lipoprotein induces endothelial progenitor cell senescence, leading to cellular dysfunction. *Clin Exp Pharmacol Physiol* 2004; 31: 407–13.
- Sacks FM, Pfeffer MA, Moye LA, Rouleau JL, Rutherford JD, Cole TG, *et al*. The effect of pravastatin on coronary events after myocardial infarction in patients with average cholesterol levels. Cholesterol and Recurrent Events Trial investigators. *N Engl J Med* 1996; 335: 1001–9.
- Asahara T, Takahashi T, Masuda H, Kalka C, Chen D, Iwaguro H, *et al*. VEGF contributes to postnatal neovascularization by mobilizing bone marrow-derived endothelial progenitor cells. *EMBO J* 1999; 18: 3964–72.
- Levadot J, Murasawa S, Kureishi Y, Uchida S, Masuda H, Kawamoto A, *et al*. HMG-CoA reductase inhibitor mobilizes bone marrow-derived endothelial progenitor cells. *J Clin Invest* 2001; 108: 399–405.
- Ma FX, Han ZC. Akt signaling and its role in postnatal neovascularization. *Histol Histopathol* 2005; 20: 275–81.
- Fulton D, Gratton JP, McCabe TJ, Fontana J, Fujio Y, Walsh K, *et al*. Regulation of endothelium-derived nitric oxide production by the protein kinase Akt. *Nature* 1999; 399: 597–601.
- Guthrie SM, Curtis LM, Mames RN, Simon GG, Grant MB, Scott EW. The nitric oxide pathway modulates hemangioblast activity of adult hematopoietic stem cells. *Blood* 2005; 105: 1916–22.
- Takemoto M, Liao JK. Pleiotropic effects of 3-hydroxy-3-methylglutaryl coenzyme a reductase inhibitors. *Arterioscler Thromb Vasc Biol* 2001; 21: 1712–9.
- Assmus B, Urbich C, Aicher A, Hofmann WK, Haendeler J, Rossig L. HMG-CoA reductase inhibitors reduce senescence and increase proliferation of endothelial progenitor cells via regulation of cell cycle regulatory genes. *Circ Res* 2003; 92: 1049–55.
- Vasa M, Fichtlscherer S, Adler K, Aicher A, Martin H, Zeiher AM, *et al*. Increase in circulating endothelial progenitor cells by statin therapy in patients with stable coronary artery disease. *Circulation* 2001; 103: 2885–90.
- Hill JM, Zalos G, Halcox JP, Schenke WH, Waclawiw MA, Quyyumi AA, *et al*. Circulating endothelial progenitor cells, vascular function, and cardiovascular risk. *N Engl J Med* 2003; 348: 593–600.
- Dimmeler S, Aicher A, Vasa M, Mildner-Rihm C, Adler K, Tiemann M, *et al*. HMG-CoA reductase inhibitors (statins) increase endothelial progenitor cells via the PI3-kinase/Akt pathway. *J Clin Invest* 2001; 108: 391–7.
- Aicher A, Heeschen C, Mildner-Rihm C, Urbich C, Ihling C, Technau-Ihling K, *et al*. Essential role of endothelial nitric oxide synthase for mobilization of stem and progenitor cells. *Nat Med* 2003; 9: 1370–6.
- Strehlow K, Werner N, Berweiler J, Link A, Dirnagl U, Priller J, *et al*. Estrogen increases bone marrow-derived endothelial progenitor cell production and diminishes neointima formation. *Circulation* 2003; 107: 3059–65.
- Shiojima I, Walsh K. Role of Akt signaling in vascular homeostasis and angiogenesis. *Circ Res* 2002; 90: 1243–50.
- Zhang Y, Lee TS, Kolb EM, Sun K, Lu X, Sladek FM, *et al*. AMP-activated protein kinase is involved in endothelial NO synthase activation in response to shear stress. *Arterioscler Thromb Vasc Biol* 2006; 26: 1281–7.
- Ju H, Zou R, Venema VJ, Venema RC. Direct interaction of endothelial nitric oxide synthase and caveolin-1 inhibits synthase activity. *J Biol Chem* 1997; 272: 18522–5.
- Laufs U, Liao JK. Post-transcriptional regulation of endothelial nitric oxide synthase mRNA stability by Rho GTPase. *J Biol Chem* 1998; 273: 24266–71.